Superposition Coded Modulation for Cooperative Communications

Hua Sun, Soon Xin Ng and Lajos Hanzo
School of Electronics and Computer Science, University of Southampton, SO17 1BJ, United Kingdom.
Tel: +44-23-8059 3125, Fax: +44-23-8059 4508
Email: {hs4g09,sxn,lh}@ecs.soton.ac.uk, http://www-mobile.ecs.soton.ac.uk

***Abstract*— A Turbo Trellis-Coded Modulation (TTCM) aided superposition modulation scheme is conceived for a Decode-and-Forward (DAF) based cooperative communication system. More specifically, two source nodes communicate simultaneously with the same destination node via a relay node. Superposition modulation is invoked at the relay node in order to combine and simultaneously transmit the two source signals to the destination node. Hence two timeslots are used to transmit two source signals. Extrinsic Information Transfer (EXIT) charts and power sharing techniques are employed in our design. The performance of the proposed scheme is investigated for transmission over uncorrelated Rayleigh fading channels, which is within about 2 dB of the corresponding capacity.**

***Index Terms*— TTCM, Superposition, Rayleigh fading channel, EXIT chart, Power Sharing**

I. INTRODUCTION

Coded Modulation (CM) [1] [2] relies on a joint design of channel coding and modulation, which absorbs the parity bits by increasing the number of bits per symbol rather than the bandwidth, as in Trellis-Coded Modulation (TCM) and Turbo Trellis-Coded Modulation (TTCM). TCM is a bandwidth efficient scheme relying on symbol-based interleaving and the classic set partitioning technique, as detailed in [1] [2] [3]. TTCM has a similar structure to turbo codes, but employs two TCM encoder/decoder blocks as its components and it performs better than TCM in both Gaussian and uncorrelated Rayleigh fading channels. The comparison of TCM, TTCM and other CM schemes such as Bit-Interleaved Coded Modulation (BICM) and BICM using Iterative Detection (BICM-ID) were discussed in [4]. In this paper, TTCM is invoked due to its superior performance in uncorrelated Rayleigh fading channels.

Cooperative communications [5] [6] constitute another effective method of combating channel fading. In this paper, a TTCM aided Decode-and-Forward (DAF) scheme is proposed. Symbol-based Super-Position Modulation (SPM) is employed at the relay node for generating a new symbol sequence, which contains all the information received from both source nodes. Hence the communication between the Relay Node (RN) and the Destination Node (DN) would only require a single timeslot. Therefore, the slot efficiency is increased and precious transmission power can be saved.

Additionally, in order to increase the attainable power efficiency of the entire DAF system, a sophisticated Power-Sharing (PS) technique based on Extrinsic Information Transfer (EXIT) charts [7] is introduced. The area under the EXIT curve is related to the normalized throughput that the decoder could reach at a given Signal-to-Noise Ratio (SNR) [8]. Hence, the EXIT chart can be used to determine the minimum SNR requited for achieving an infinitesimally low Bit Error Ratio (BER). In this paper, the entire relaying system is divided into two links, namely the source-to-relay (SR) link and the relay-to-destination (RD) link. The minimum required SNR of each link is different. Hence, if the transmission power of the Source Nodes (SNs) and that of the RN were constrained to be identical, this would degrade the power efficiency of the whole system. An appropriate PS technique is capable of rearranging the transmission power of each SN and RN node, so that both the RN and DN simultaneously achieve an infinitesimally low BER. Hence, the BER performance of the system can be improved at a given average transmission power, when the appropriate PS technique is employed.

The financial support of the EPSRC UK under the auspices of the China-UK Science Bridge, the India-UK Advanced Technology Centre and that of the European Union's Seventh Framework Programme (FP7/2007-2013) under the auspices of the CONCERTO project (grant agreement no 288502) is greatly appreciated.

The contributions of this paper are:

1) The TTCM channel coding scheme was combined with the SPM technique to improve the performance of a two-user cooperative communication system and the detailed design was presented.
2) The PS technique was brought in and the power efficiency of the entire system had been improved.

The organisation of this paper is as follows. Section II presents the system model and our motivation. Section III illustrates the SPM mapping at the RN, while Section V details the detection of the super-symbols. The pathloss reduction and our PS technique are detailed in Section VI. Our simulation results and analysis are provided in Section VII, while our conclusions are offered in Section VIII.

II. SYSTEM MODEL

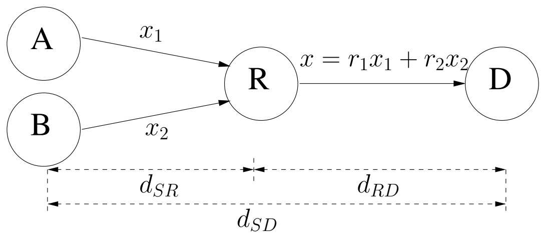

Fig. 1. The model of two SNs, one RN and one DN cased system.

Fig. 1 shows our system model. Two SNs, namely A and B, communicate with the DN labelled as D using the RN denoted as R. The signal received at the DN is given by:

$$y = hx + n \ , \tag{1}$$

where h is the complex-valued channel fading coefficient and n is the Additive White Gaussian Noise (AWGN) having a variance of $N_0/2$ per dimension, while x is the SPM super-symbol generated from x_1 and x_2, which would be detailed in Eq. (2).

If the RN receives two frames of 4PSK signals from two SNs during the first two timeslots and re-transmits them to the DN using another two timeslots, then this protocol would require four timeslots for conveying information from the SNs to the DN. However, this is wasteful in terms of slot-bandwidth-and-power-efficiency. If the RN

978-1-4673-1881-5/12/$31.00 ©2012 IEEE

generates 16QAM symbols based on the information contained in the 4PSK signals received from the two SNs, then it will only take three timeslots for the DN to receive the two information frames from the SNs. However, a higher order modulation scheme typically imposes a higher complexity and a reduced fading resistance, which would lead to a poor BER performance. Here we conceive a SPM aided MIMO technique for the RN, where the RN firstly simultaneously receives the signals from the two SNs during the first timeslot. Then, the RN decodes and re-encodes the two symbols using the same number of modulation levels. As shown is Eq. (2), the two signal frames would then be linearly combined using different weighting factors to generate a super-symbol frame, which would be transmitted to the DN during the second timeslot. In this case, it would only require two timeslots for transmitting two information frames from the two SNs to the DN.

III. Low Order Linear Superposition

The SPM scheme was introduced in [5] [9]. Fig. 2 shows the generation of the super-symbols. It can be seen that the constellation map of the super-symbol is similar to that of a 16QAM scheme. An SPM weighting factor pair (r_1,r_2) is defined, where r_1 is assigned to x_1, which is the symbol received from SN A, while r_2 is assigned to x_2, which is the symbol received from SN B. Then the SPM symbol can be written as:

$$x = r_1 x_1 + r_2 x_2 \ , \tag{2}$$

where we have $E[|x_1|^2] = 1$ and $E[|x_2|^2] = 1$, since the average symbol power is assumed to be unity. When the two 4PSK symbols are multiplied using their SPM weighting factors, their average power becomes:

$$E\left[\mid r_1 \mathbf{x_1} \mid^2\right] = {r_1}^2 E\left[\mid \mathbf{x_1} \mid^2\right] = {r_1}^2 \ , \tag{3}$$

$$E\left[\mid r_2 \mathbf{x_2} \mid^2\right] = {r_2}^2 E\left[\mid \mathbf{x_2} \mid^2\right] = {r_2}^2 \ . \tag{4}$$

Since the average symbol power of the super-symbol should also be unity, we have:

$$\begin{aligned} E\left[\mid \mathbf{x} \mid^2\right] &= E\left[\mid r_1\mathbf{x_1} + r_2\mathbf{x_2} \mid^2\right] \\ &= E\left[{r_1}^2{\mathbf{x_1}}^2 + {r_2}^2{\mathbf{x_2}}^2 + 2r_1r_2\mathbf{x_1}\mathbf{x_2}\right] \\ &= {r_1}^2 E\left[\mid \mathbf{x_1} \mid^2\right] + {r_2}^2 E\left[\mid \mathbf{x_2} \mid^2\right] + 2r_1r_2E\left[\mathbf{x_1}\mathbf{x_2}\right] \\ &= {r_1}^2 + {r_2}^2 + 2r_1r_2E\left[\mathbf{x_1}\mathbf{x_2}\right] \\ &= 1 \ . \end{aligned} \tag{5}$$

Furthermore, the two 4PSK symbol streams are independent of each other, yielding:

$$E\left[\mathbf{x_1}\mathbf{x_2}\right] = E\left[\mathbf{x_1}\right]E\left[\mathbf{x_2}\right] = 0 \ , \tag{6}$$

where we have $E\left[\mathbf{x_1}\right] = E\left[\mathbf{x_2}\right] = 0$. Hence, it can be seen that the SPM weighting factor pair should satisfy:

$${r_1}^2 + {r_2}^2 = 1 \ . \tag{7}$$

It may be observed from the Fig. 2 that if the factor r_1 is larger than r_2, the constellation map of the super-symbol would be the expansion of the constellation map of x_2 based on the constellation map of x_1. Here we define x_1 to be the dominant symbol and x_2 to be the auxiliary symbol. As shown in Fig. 2, the minimal Euclidean distance d among the super-symbols is decided by the distance of d_1 and d_2 in Fig. 2, which may be derived based on the value of r_1, where d is given by:

$$d = \begin{cases} \frac{1}{\sqrt{2}} \min\left(2\sqrt{1-{r_1}^2}, 2\left(r_1 - \sqrt{1-{r_1}^2}\right)\right) & \left(r_1 \geq \sqrt{1/2}\right) \\ \frac{1}{\sqrt{2}} \min\left(2r_1, 2\left(\sqrt{1-{r_1}^2} - a\right)\right) & \left(r_1 < \sqrt{1/2}\right) \ . \end{cases} \tag{8}$$

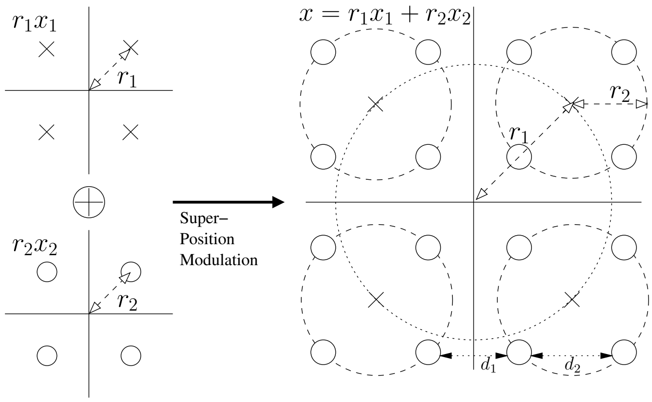

Fig. 2. The generation of a 16-level super symbol set from two 4PSK symbol sets.

If $r_1 \geq \sqrt{1/2}$, the maximum minimal Euclidean distance $d_{\max}$ is achieved for $2\sqrt{1-{r_1}^2} = 2(r_1 - \sqrt{1-{r_1}^2})$, which gives $r_1 = \sqrt{4/5}$. By contrast, if $r_1 < \sqrt{1/2}$, then $d_{\max}$ is attained for $2r_1 = 2(\sqrt{1-{r_1}^2} - r_1)$, which gives $r_1 = \sqrt{1/5}$. The minimal Euclidean distance $d_{\max}$ within the constellation map of the superposition symbols would be maximised, when r_1 equals to $\sqrt{1/5} = 0.4472$ or $\sqrt{4/5} = 0.8944$. The weighting factor pair (0.4472, 0.8944) also obeys Eq. (7), which is the optimum choice in terms of maximising the minimal Euclidean distance. Naturally, a higher minimal Euclidean distance in a constellation set implies having a higher resistance against channel fading and noise. Note that a super-symbol is the combination of the dominant symbol and the auxiliary symbol, where the dominant symbol has a larger minimal Euclidean distance, hence exhibiting in an improved BER performance compared to that of the auxiliary symbol. Therefore, a strategy was required to balance these two BERs which will be proposed in Section VII.

IV. Detection of the Super-symbols

In the RN, two 4PSK symbol sequences are merged to form a SPM signal sequence. Although the new super-symbol contains the information of two 4PSK symbols and the constellation map of the superposition signal is similar to 16QAM, the decoding block of the receiver is still based on 4PSK symbols. The soft decoder needs the symbol probabilities for decoding, based on the constellation map and the received SPM symbol. The first step is to detect the symbol probabilities of the super-symbol and then compute the symbol probabilities of the two 4PSK symbol sequences.

The probability of receiving y given that the super-symbol $x = r_1x_1 + r_2x_2$ was transmitted is expressed as:

$$P(y|x_1,x_2) = \frac{1}{\pi N_0} \exp\left(-\frac{\left|y - h\left(r_1x_1 + r_2x_2\right)\right|^2}{N_0}\right) \ . \tag{9}$$

The symbol probabilities for x_1 and x_2 may be derived from Eq. (9) as:

$$P(y|x_1 = x^{(i)}) = \sum_{k=0}^{3} P\left(y|x_1 = x^{(i)}, x_2 = x^{(k)}\right) \ , \tag{10}$$

$$P(y|x_2 = x^{(k)}) = \sum_{i=0}^{3} P\left(y|x_2 = x^{(k)}, x_1 = x^{(i)}\right) \ , \tag{11}$$

where $x^{(i)}$ and $x^{(k)}$ are the hypothetically transmitted 4PSK symbols for $\{i,k\} \in \{0,1,2,3\}$. Then, the TTCM decoder of the DN recovers the two information sequences based on Eq. (10) and Eq. (11).

V. ITERATIVE DECODING AND EXIT CHART ANALYSIS

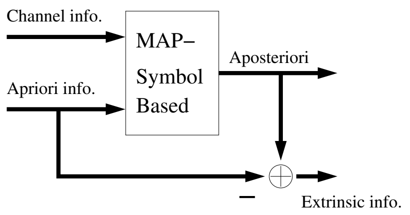

Fig. 3. The TCM decoder [2] constitutes a Maximum Aposteriori Probability (MAP) based decoder.

The iterative decoding of TTCM was detailed in [2] [10]. A TTCM decoder is constituted by a pair of TCM decoders, as shown in Fig. 3, while, Fig. 4 shows the iterative information exchange between the TTCM decoder and the demapper at the RN. The detection is based on an equivalent two-transmitter one-receiver system. The EXIT chart visualises the extrinsic information flow between the two TCM decoders and the Soft-Demapper [7] [11]. The two TCM decoders are identical. As observed in Fig. 4 that the probability of the codeword $P_a(c)$ gleaned from the Soft-Demapper is not the only input. The other input $P_a(d)$ is received from the lower TCM decoder, which is the probability of the dataword. Both $P_a(c)$ and $P_a(d)$ are used for generating the aposteriori information (APP) of the dataword $P_o(d)$. After subtracting the apriori information $P_a(d)$ from the aposteriori information $P_o(d)$, the extrinsic probability of the dataword $P_e(d)$ is obtained. Then, $P_e(d)$ is interleaved to generate the apriori information $P_a(d)$ for the lower TCM decoder. The same process is repeated at the lower TCM decoder, except that the lower TCM decoder would additionally compute the aposteriori probability of the codeword $P_o(c)$ during the last TCM iteration. The interleaver and de-interleaver between the two TCM decoders will not influence the amount of mutual information, its role is to keep the sequence of the two data streams in the right order. As shown in Fig. 4, the probability of the codeword $P_o(c)$ at the output of the lower TCM decoder would be fed to the Soft-Demapper, while $P_o(d)$ would be forwarded to the decision block.

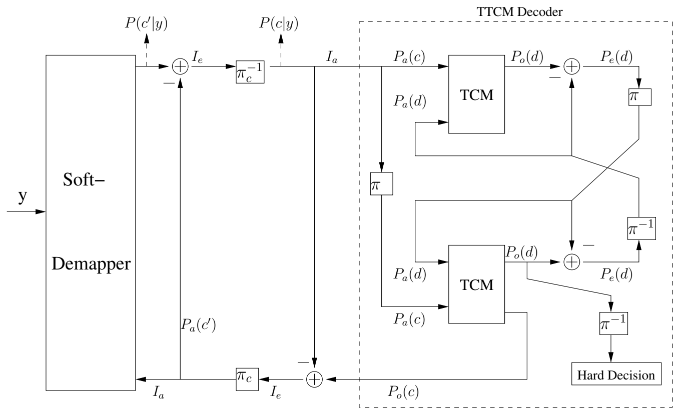

Fig. 4. The detection block diagram at the RN.

Fig. 5 shows the EXIT chart characterising the extrinsic information exchange between the TTCM decoder and the MIMO-2X1 demapper. More specifically, the outer decoder's EXIT curve is based on the apriori information $P_a(c)$, while the extrinsic information is $[P_o(d) - P_a(d)]$, which is the input and output of the TTCM decoder block in Fig. 4. Hence, the shape of this curve is dependent on the number of TTCM iterations and on the component TCM decoder. By contrast, the inner decoder's EXIT curve is based on the apriori information in $P_a(c')$ and on the extrinsic information $[P(c'|y) - P_a(c')]$. The inner decoder's EXIT curve is also dependent on the SNR.

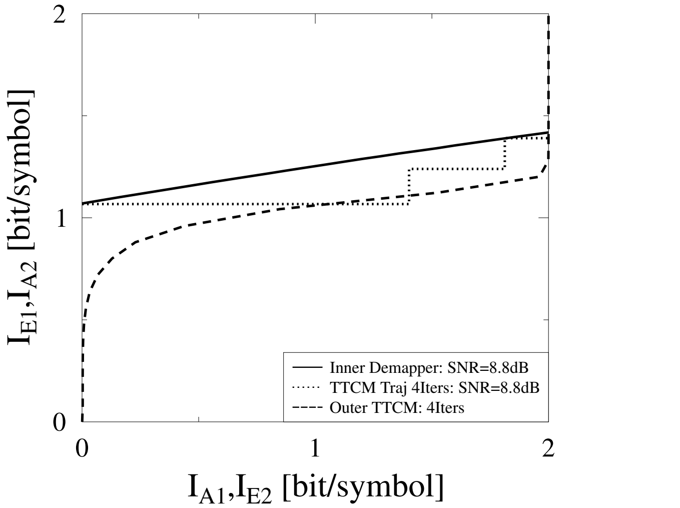

Fig. 5. EXIT chart based on MIMO-2x1 assisted TTCM 4PSK scheme, when communicating over uncorrelated Rayleigh fading channel. The block length is 12000 symbols and the number of TTCM iterations is 4.

Based on a given number of modulation levels, on the SNR and on the number of iterations, an open EXIT tunnel leading to the (2,1) point of Fig. 5 might be formed. When this is the case, decoding convergence to an infinitesimally low BER is possible. The step-wise linear decoding trajectory traversing through the open EXIT chart tunnel of Fig. 5 is based on Monte-Carlo simulations. It depicts the information exchange during each iteration between the MIMO-2X1 demapper and the TTCM decoder. The variables I_a and I_e in the EXIT charts represent all the mutual information terms in units of bits per symbol. The maximum mutual information value in the EXIT chart is $I_e = 2$, because 4PSK modulation is employed. Again, the EXIT charts can be used to find the minimum SNR required for achieving an infinitesimally low BER. The PS technique can be invoked to reduce the overall transmission power.

VI. PATH GAIN AND POWER SHARING

A Path Gain

As shown in Fig. 1, when relying on a RN, the propagation distance d_{SD} is divided into two parts, namely d_{SR} and d_{RD}, hence the path loss is reduced and the performance of the system may be improved. When considering an inverse-square-power free-space path loss model, the reduced-distance-related pathloss reduction (path gain) between the SN and RN can be expressed as [12]:

$$g_{sr} = \frac{d_{sd}^2}{d_{sr}^2} \ , \tag{12}$$

$$G_{sr} = 10 \log_{10} (g_{sr}) \, [dB] \ . \tag{13}$$

By contrast, the path gain of the link between the RN and the DN is

$$g_{rd} = \frac{d_{sd}^2}{d_{rd}^2} \ , \tag{14}$$

$$G_{rd} = 10 \log_{10} (g_{rd}) \, [dB] \ . \tag{15}$$

If the RN is located right in the middle, then we have $d_{SR} = d_{RD} = d_{SD}/2$ and $G_{sr} = G_{rd} \approx 6.02\ dB$.

B Power Sharing

In this section optimum PS is proposed for reducing the overall transmission power of the whole system. To achieve an infinitesimally low BER (eg. 10^{-7}), the required receive SNR (dB) of the RN is different from that of the DN. In this situation, optimally sharing the overall average transmission power between the SNs and RN based on the difference between the receive SNR required at the RN and at the DN is capable of increasing the power efficiency of the entire system. When considering the path gain, if the transmission power ratio (SNR ratio) required to get a low BER at the SN is denoted as $\gamma_{T,s}$ and that of the RN is as $\gamma_{T,r}$, then we have:

$$\Upsilon_{R,r} = 10\log_{10}(\gamma_{T,s}) + G_{sr}[dB] \ , \quad (16)$$

$$\Upsilon_{R,d} = 10\log_{10}(\gamma_{T,r}) + G_{rd}[dB] \ , \quad (17)$$

where, $\Upsilon_{R,r}$ and $\Upsilon_{R,d}$ is the receive SNR (dB) required at the RN and DN, respectively. Based on Eq. (16) and Eq. (17), if the difference of the receive SNR (dB) required between the RN and DN is represented by $\Upsilon_{R,\Delta}$, then we have:

$$\begin{aligned}\Upsilon_{R,\Delta} &= \Upsilon_{R,d} - \Upsilon_{R,r} \\ &= 10\log_{10}(\gamma_{T,r}) - 10\log_{10}(\gamma_{T,s}) \\ &= 10\log_{10}\left(\frac{\gamma_{T,r}}{\gamma_{T,s}}\right) \ . \end{aligned} \quad (18)$$

If $\Upsilon_{R,\Delta} = 10\log_{10}(\gamma_{R,\Delta})$, then the receive SNR ratio between the RN and DN may be formulated as:

$$\gamma_{R,\Delta} = \frac{\gamma_{T,r}}{\gamma_{T,s}} \ , \quad (19)$$

where the average transmission power ratio per timeslot of the overall system is given by:

$$\bar{\gamma}_T = \frac{\gamma_{T,s} + \gamma_{T,r}}{2} \ . \quad (20)$$

Hence, the transmission power ratio at the SNs can be formulated as:

$$\gamma_{T,s} = \frac{2\bar{\gamma}_T}{1+\gamma_{R,\Delta}} \ , \quad (21)$$

while, the transmission power ratio at the RN is given by:

$$\gamma_{T,r} = \frac{2\bar{\gamma}_T\gamma_{R,\Delta}}{1+\gamma_{R,\Delta}} \ . \quad (22)$$

VII. Simulation results

The BER versus SNR performance of the SPM aided TTCM-4PSK scheme communicating over uncorrelated Rayleigh fading channels is shown in Fig. 6 and Fig. 7. The performance of the first user is studied when using an SPM weighting factor r_1 ranging from 0.1 to 0.95. As seen in Fig. 6 and Fig. 7, when r_1 increases, the performance of the first user improves, except for $r_1 = 0.707$. When we have $r_1 = 0.707$, the 16-point SPM constellation of Fig. 2 will collapse into a 9-point SPM constellation, because some of the constellation points are at the same location. This would make detection impossible and a high BER floor will emerge. Note that for $r_1 > 0.7071$ the first user's signal x_1 becomes the dominant signal, while x_2 becomes the auxiliary signal, where we have $r_2 < 0.707$, and vice versa. The higher r_1 , the stronger protection the dominant symbol x_1 will have, which directly leads to a performance loss for the auxiliary symbol x_2. As seen in Fig. 6, the best ratio for the auxiliary signal is given by 0.4472. According to the analysis of Section III, the optimum SPM weighting factor pair is given by [0.4472,0.8944].

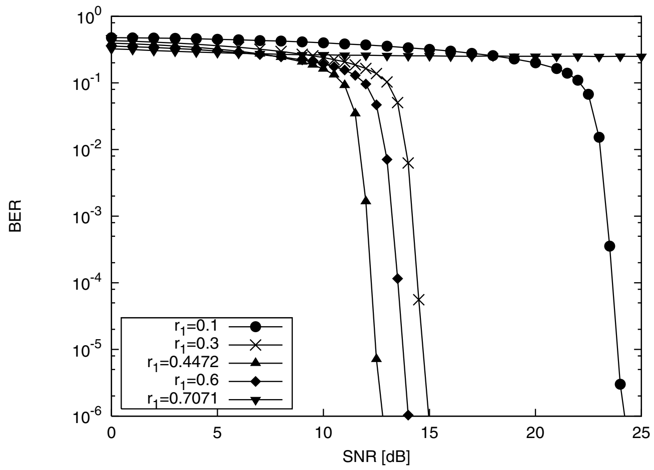

Fig. 6. The BER versus SNR performance of the SPM aided TTCM-4PSK scheme, when communicating over uncorrelated Rayleigh fading channels. The performance of the first user is studied when using a ratio factor of $r_1 = \{0.1, 0.3, 0.4472, 0.6, 0.707\}$. A block length of 12 000 symbol is employed and the number of TTCM iterations is fixed to four.

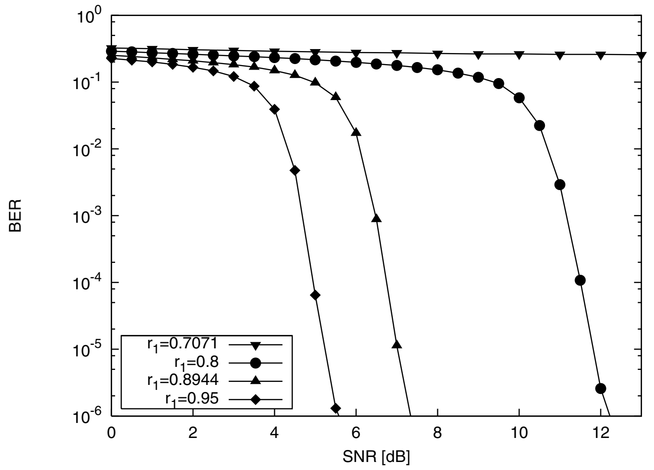

Fig. 7. The BER versus SNR performance of the SPM aided TTCM-4PSK scheme, when communicating over uncorrelated Rayleigh fading channels. The performance of the first user is studied when using a ratio factor of $r_1 = \{0.707, 0.8, 0.8944, 0.95\}$. A block length of 12 000 symbol is employed and the number of TTCM iterations is fixed to four.

We have proposed the 'Equal BER' method to achieve the same BER for both users by using [0.4472,0.8944] for all even symbol periods, while swapping the weighting factor to [0.8944,0.4472] for all odd symbol periods. The performance of the Equal BER scheme is shown in Fig. 8 in comparison to the user 1 and user 2 performance curves based on the fixed ratio factor pair of (0.8944,0.4472). As seen in Fig. 8, the performance of the Equal BER method is approximately 2.4 dB better than that of user 2, but approximately 3 dB worse than that of user 1 for the conventional method at a BER of 10^{-6}. Moreover, the RN could also absorb the two information bits contained in the two 4QAM symbols and communicate with DN by 8PSK symbol with code rate 2/3. In this situation, the modulation level at the RN and the DN is increased from 4 to 8, while its BER performance is approximately 3 dB worse than that of our equal BER scheme at a BER of 10^{-6}, as shown in Fig. 8.

Fig. 5 shows the EXIT chart for the detection at the RN, where two SNs simultaneously transmit their 4PSK-based frames to

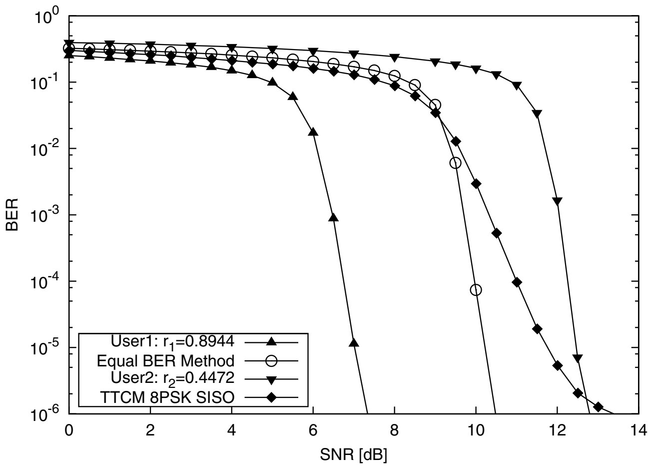

Fig. 8. The BER versus SNR performance of the SPM aided TTCM-4PSK scheme, when communicating over uncorrelated Rayleigh fading channels. The performance curves of the first and second users are based on the ratio factors of $r_1 = 0.8944$ and $r_2 = 0.4472$, respectively. The equal BER method is also considered for comparison. A block length of 12 000 symbol is employed and the number of TTCM iterations is fixed to four.

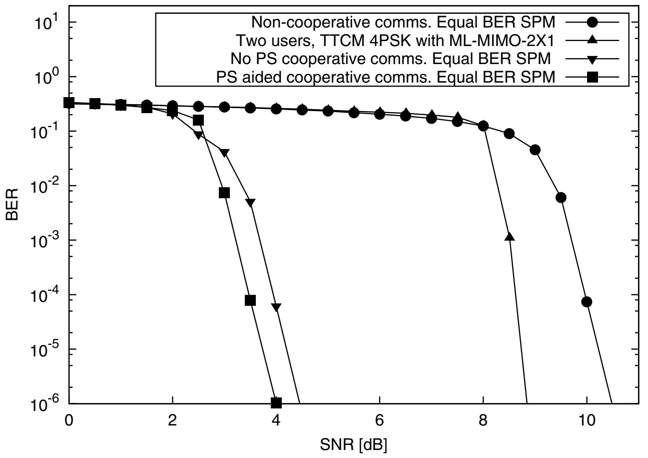

Fig. 9. The BER versus SNR performance of the SPM aided TTCM-4PSK based cooperative communication schemes, when communicating over uncorrelated Rayleigh fading channels. The performance curves of the non-cooperative SPM aided TTCM-4PSK scheme and of the MIMO-2X1 aided TTCM-4PSK scheme are also considered for comparisons. A block length of 12 000 symbol is employed and the number of TTCM iterations is fixed to four.

the RN. This is equivalent to a MIMO-2x1 scheme, where two transmit antennas are used for conveying two independent signals to a receiver having a single antenna. The number of TTCM decoding iterations was fixed to four. As seen in Fig. 5, the link between the SNs and the RN requires an SNR of 8.8 dB in order to achieve a low BER at the RN. By contrast, as seen in Fig. 8, the RN to DN link requires an SNR of 10.5 dB to achieve a BER below 10^{-6}. The difference between these two SNRs is given by $\Upsilon_{R,\Delta} = 10.5 - 8.8 = 1.7$ dB, which is required by the PS technique for improving the overall power-efficiency of the system. Our simulation results recorded for the TTCM-4PSK aided SPM based cooperative schemes are depicted in Fig. 9. When a RN located at the midway position between the SNs and DN is employed, the PS based scheme performs approximately 0.5 dB better than the equal-power scheme at a BER of 10^{-6}. As seen in Fig. 9, it can be stated that the PS-based SPM cooperative scheme requires approximately $10.5 - 4.0 = 6.5$ dB lower SNR than the non-cooperative SPM scheme. It is also $8.8 - 4.0 = 4.8$ dB more power-efficient than the two-transmitter one-receiver TTCM-4PSK scheme.

VIII. Conclusions

We have conceived a SPM based TTCM aided scheme for cooperative communications. The proposed scheme only requires two timeslots to convey two information frames from two SNs to the DN. Both EXIT charts and PS techniques were employed for increasing the power efficiency of the entire cooperative communication system. We demonstrated that the proposed scheme only requires approximately 4.0 dB to achieve a BER of 10^{-6}, which is about 6.5 dB lower than the SNR required by the non-cooperative SPM scheme. We have also proposed a SPM scheme capable of providing an identical BER for both signal sets. Hence, the employment of an appropriate by designed SPM at the RN improved both the bandwidth-and-power-efficiency of the system.

References

[1] G. Ungerböck, "Trellis-coded modulation with redundant signal sets. Part 1 and 2," *IEEE Communication Magazine*, vol. 25, pp. 5–21, February 1987.

[2] L. Hanzo, T. H. Liew, B. L. Yeap, R. Y. S. Tee, S. X. Ng , *Turbo coding, turbo equalization and space-time coding EXIT-Chart aided near-capacity designs for wireless channels*. John Wiley and Sons, 2 ed., 2011.

[3] D. Divsalar and M. K. Simon, "The design of trellis coded MPSK for fading channel: set partitioning for optimum code design," *IEEE Transactions on Communications*, vol. 36, pp. 1015–1019, September 1988.

[4] S. X. Ng, T. H. Liew, L.-L. Yang and L. Hanzo, "Comparative study of TCM, TTCM, BICM and BICM-ID schemes," *in IEEE Vehicular Technology Conference, (Rhodes, Greece)*, pp. 2450–2454, May 2010.

[5] S. Huan, Z. Fei, L. Huang, J. Kuang , "Cooperative transmission utilizing high order superposition modulation with iterative detection," *IEEE Communications Letters*, pp. 1 – 5, 24-26 Sept 2009.

[6] S. X. Ng, K. Zhu and L. Hanzo, "Distributed source-coding, channel-coding and modulation for cooperative communication," *Vehicular Technology Conference Fall (VTC 2010-Fall), 2010 IEEE 72nd* , September 2010.

[7] S. X. Ng, Y. Li, J. Kliewer and L. Hanzo, "Near-capacity Turbo Trellis Coded Modulation design based on EXIT charts and union bounds," *Communications, IEEE Transactions*, vol. 56, pp. 2030–2039, December 2008.

[8] S. X. Ng, J. Wang, L. Hanzo, "Unveiling near-capacity code design: the realization of shannon's communication theory for MIMO channels," *Communications, 2008. ICC '08. IEEE International Conference* , pp. 1415 – 1419 , May 2008 .

[9] L. Huang, Z. Fei, J. Kuang , "A decode-and-forward relaying scheme based on orthogonal superposition modulation," *Communication Technology,IEEE International Conference*, pp. 241–244, 10-12 Nov 2008.

[10] P. Robertson and T. Worz, "Band-Efficient Turbo Trellis-Coded Modulation using punctured component Codes," *IEEE Journal on Selected Areas in Communications*, vol. 16, February 1998.

[11] J. Kliewer, S. X. Ng and L. Hanzo, "Efficient computation of exit functions for non-binary iterative decoding," *IEEE Transactions on Communications*, vol. 54, pp. 2133–2136, December 2006.

[12] H. Ochiai, P. Mitran and V. Tarokh, "Design and analysis of collaborative diversity protocols for wireless sensor networks," *Vehicular Technology Conference, 2004. VTC2004-Fall. 2004 IEEE 60th* , vol. 7, pp. 4645–4649, Sep 2004.